### Title

Tobacco toxins deposited on surfaces (third hand smoke) impair wound healing.




### Journal

Clinical Science, 130(14)

### ISSN

0143-5221



### Authors

Dhall, Sandeep

Alamat, Raquelle

Castro, Anthony

et al.



### Publication Date

2016-07-01

### DOI

10.1042/cs20160236

Peer reviewed

Clinical Science (2016) **130**, 1269–1284 doi: 10.1042/CS20160236

**Original Paper**

# Tobacco toxins deposited on surfaces (third hand smoke) impair wound healing

Sandeep Dhall*, Raquelle Alamat*, Anthony Castro*, Altaf H. Sarker†, Jian-Hua Mao†, Alex Chan*, Bo Hang† and Manuela Martins-Green*

*Department of Cell Biology and Neuroscience, University of California at Riverside, Riverside, CA 92521, U.S.A.
†Biological Systems & Engineering Division, Lawrence Berkeley National Laboratory, Berkeley, CA 94720, U.S.A.

## Abstract

Third hand smoke (THS) is the accumulation of second hand smoke (SHS) toxins on surfaces in homes, cars, clothing and hair of smokers. It is known that 88M US nonsmokers $\geqslant$3 years old living in homes of smokers are exposed to THS toxicants and show blood cotinine levels of $\geqslant$0.05 ng/ml, indicating that the toxins are circulating in their circulatory systems. The goal of the present study is to investigate the mechanisms by which THS causes impaired wound healing. We show that mice living under conditions that mimic THS exposure in humans display delayed wound closure, impaired collagen deposition, altered inflammatory response, decreased angiogenesis, microvessels with fibrin cuffs and a highly proteolytic wound environment. Moreover, THS-exposed mouse wounds have high levels of oxidative stress and significantly lower levels of antioxidant activity leading to molecular damage, including protein nitration, lipid peroxidation and DNA damage that contribute to tissue dysfunction. Furthermore, we show that elastase is elevated, suggesting that elastin is degraded and the plasticity of the wound tissue is decreased. Taken together, our results lead us to conclude that THS toxicants delay and impair wound healing by disrupting the sequential processes that lead to normal healing. In addition, the lack of elastin results in loss of wound plasticity, which may be responsible for reopening of wounds.

**Key words:** angiogenesis, cytokine, DNA damage, inflammation, reactive oxygen species and antioxidants, toxicants.

## INTRODUCTION

Wound healing is a dynamic process involving many factors and cell types including soluble mediators, blood cells, fibroblasts, endothelial cells and extracellular matrix [1]. Injury initiates a cascade of repair processes that normally begins with blood clotting, followed by a variety of oxidative and nitro-oxidative reactions. Normal cutaneous wound healing is divided into several sequential but overlapping phases in space and time – homoeostasis, inflammation, granulation tissue formation and tissue remodelling – that must occur in an orderly manner to achieve proper healing. Impaired and chronic wounds result from an imbalance in the healing cascade and have a significant impact on human health [2].

Cigarette smoke is a complex mixture of more than 7000 toxic substances [3]. Third hand smoke (THS) is created by the recurring deposition of tobacco toxins on curtains, carpet, upholstery, bedding, windows and walls of buildings; and in vehicles, on car seats and other interior surfaces. It also lingers in smokers' hair, clothing and skin [4,5]. The chemical conversion of second hand smoke (SHS) into THS is a dynamic aging process that begins within 30 min of smoking. This causes THS to become more toxic and potentially more harmful than fresh SHS with time [6]. Contamination of the homes of smokers by SHS residues (i.e. THS) is high, both on surfaces and in dust, including in children's bedrooms. Recently, it has also been shown that THS remains in houses and apartments even long after the smokers move out [7]. This makes THS a serious health risk – a stealth toxin – especially for children and the elderly who are more vulnerable to these toxins than adults [8–10] and are unable to remove themselves from these environments.

Although doctors require patients to refrain from smoking before scheduled surgery and have suggested beneficial effects due to abstinence [11,12], reports have also suggested that short

**Abbreviations:** FACS, fluorescence activated cell sorting; GCSF, granulocyte colony stimulating factor; GPx, glutathione peroxidase; GR, glutathione reductase; IACUC, Institutional Animal Care and Use Committee; LA-qPCR, large Amplicon quantitative PCR; LIF, leukaemia inhibitory factor; MCP-1, monocyte chemoattractant protein; MDA, malondialdehyde; MIP-1$\alpha$, macrophage inflammatory protein 1$\alpha$; MMP, matrix metalloproteinase; 3-NT, 3-nitrotyrosine; 8-OH-dG, 8-hydroxy-2-deoxy guanosine; pol$\beta$, polymerase $\beta$; ROS, reactive oxygen species; SHS, second hand smoke; $\alpha$SMA, $\alpha$-smooth muscle actin; SOD, superoxide dismutase; TBARS, thiobarbituric acid reactive substances; THS, third hand smoke; TIMP, tissue inhibitors of matrix metalloproteinase.

**Correspondence:** Manuela Martins-Green (email manuela.martins@ucr.edu).

 

term cessation of smoking does not effectively reduce the risk and complications during wound healing after surgery [13]. Because THS toxins can affect infants, children and elderly, who are defenseless to that exposure, understanding the detrimental effects of THS on wound healing is important in identifying the risks associated with the residual toxicants left from SHS and those resulting from changes occurring due to interactions with the environment that contribute to formation of THS.

We have recently developed an animal model system that mimics human exposure to THS. Our studies showed significant damage to liver, lung and cognitive behaviour [14]. Furthermore, THS was also shown to cause delayed healing [14]. However, the cell and molecular mechanisms associated with the development of impaired wounds has not been studied. Thus, the goal of the present study is to investigate the mechanisms by which THS causes impaired wound healing. In the present study we show that wounds of THS-exposed mice close at a slower rate than those of control mice and that they have problems in epithelial migration, collagen deposition and granulation tissue formation. We also show problems in oxidative stress, inflammation, chemokine/cytokine production and angiogenesis, all of which are major components of a healthy regenerative tissue healing process. Our findings in the present study delineate the impact of THS on wound healing processes in mice and suggest the occurrence of similar problems in humans exposed to THS.

## RESEARCH DESIGN AND METHODS

### Animals

All animal experiments were approved by the University of California, Riverside, Institutional Animal Care and Use Committee (IACUC). Methodology used was as previously described [14]. Briefly, C57BL/6 mice were divided into control and THS-exposed mice with exposure starting right after weaning and proceeding until 24 weeks of age. All mice were fed a standard chow diet (percent calories: 58% carbohydrate, 28.5% protein and 13.5% fat).

### THS exposure

Using the previously established THS exposure system [14], common household fabrics were placed in mouse cages and subjected to SHS cigarette smoke. Briefly, each cage contained 10 g of curtain material (cotton), 10 g of upholstery (cotton and fibre) and 2.16 $in^2$ pieces of carpet (fibre), in order to maintain equal exposure levels across experimental groups. Two packs of 3R4F research cigarettes were smoked each day, 5 days/week and smoke was routed to a mixing compartment and distributed between two exposure chambers containing cages with the materials. The total particulate matter (TPM) was monitored twice daily and kept at $30 \pm 5\ \mu g/m^3$. All cigarettes were smoked and stored in accordance with the FTC smoking regimen. Mice were then placed into cages containing materials that had been smoked for a week.

### Dermal excision wound model

C57BL/6 mice exposed and not exposed to THS (Jackson Laboratories) were housed in the UCR vivarium and were treated following protocols approved by the IACUC. The wounds were performed as we previously described [15]. Briefly, dorsal hair was removed using clippers and nair on control and THS-exposed mice. 24 h later, full thickness excision wounds were performed on the dorsum of the mice using a 7 mm biopsy punch (Acuderm). Wound tissues were collected at various time points following injury using a 10 mm diameter biopsy punch.

Tissue extracts were prepared as previously described by us [16].

### Superoxide dismutase activity assay

Total tissue superoxide dismutase (SOD) activity was measured using a commercially available kit (Cayman Chemical) that measures all three types of SOD (Cu/Zn-, Mn- and EC-SOD). One unit of SOD is defined as the amount of enzyme needed to cause 50% dismutation of the superoxide radical. The SOD activities of the samples were calculated from the linear regression of a standard curve that was determined using the SOD activity of bovine erythrocytes at various concentrations run under the same conditions. The SOD activity was expressed as unit/ml of tissue extract.

### Hydrogen peroxide activity assay

Tissue hydrogen peroxide ($H_2O_2$) levels were measured using a commercially available kit (Cell Technology) that utilizes a non-fluorescent detection reagent. The assay is based on the peroxidase-catalysed oxidation by $H_2O_2$ of the nonfluorescent substrate 10-acetyl-3,7-dihydroxyphenoxazine to a fluorescent resorufin. Fluorescent intensities were measured at 530 nm (excitation)/590 nm (emission) using a Victor 2 microplate reader. The levels of $H_2O_2$ in the supernatants were derived from a seven-point standard curve generated with known concentrations of $H_2O_2$.

### Catalase activity assay

Tissue catalase activity was measured using a commercially available kit (Cayman Chemical). The enzyme assay for catalase is based on the peroxidatic function of catalase with methanol to produce formaldehyde in the presence of an optimal concentration of $H_2O_2$. The formaldehyde produced was measured spectrophotometrically with 4-amino-3-hydrazino-5-mercapto-1,2,4-triazole (purpald) as the chromogen at 540 nm in a 96-well plate. The catalase activity was expressed as nmol/min per ml of tissue extract.

### Glutathione peroxidase activity assay

Tissue glutathione peroxidase (GPx) activity was measured using a commercially available kit (Cayman Chemical). The activity was measured indirectly by a coupled reaction with glutathione reductase (GR). GPx reduces $H_2O_2$ to $H_2O$ and in the process oxidized glutathione (GSSG) is produced that in turn is recycled to its reduced state by GR and NADPH. Furthermore, oxidation of NADPH to $NADP^+$ is accompanied by a decrease in absorbance at 340 nm. Under conditions in which GPx activity is rate limiting, the rate of decrease in the absorbance measured at 340 nm, in a 96-well plate at 1-min interval for a total of 5 min using a Victor 2 microplate reader, is directly proportional to the GPx

 

activity of the sample. GPx activity was expressed as nmol/min per ml of tissue extract.

### Lipid peroxidation assay using thiobarbituric acid reactive substances

Tissue thiobarbituric acid reactive substances (TBARS) were measured by using a commercially available kit (Cell Biolabs). Lipid peroxidation results in unstable lipid peroxides that further decompose into natural byproducts such as malondialdehyde (MDA) and 4-hydroxynonenal (4-HNE). MDA forms adducts with TBARS in a 1:2 proportion. These adducts were measured fluorometrically at an excitation of 540 nm and emission at 590 nm. TBARS levels were then calculated in $\mu$M by comparison with a predetermined MDA standard curve.

### Nitrotyrosine ELISA

Tissue nitrotyrosine levels were measured by using a commercially available kit (Cell Biolabs). The measurements are based on a competitive enzyme immunoassay. The tissue sample or nitrated BSA were bound to an anti-nitrotyrosine antibody, followed by an horseradish peroxidase conjugated secondary antibody and enzyme substrate. The absorbance was measured spectrophotometrically at 412 nm and the nitrotyrosine content in the unknown sample was then determined by comparing with a standard curve that was prepared from predetermined nitrated BSA standards.

### Isolation of DNA and 8-hydroxy-2-deoxy guanosine analysis

Tissue DNA was extracted by using a commercially available kit (Qiagen). Eluted DNA was digested using nuclease P1 and the pH adjusted to 7.5–8.5 using 1 M Tris. The DNA was incubated for 30 min at 37 °C with 1 unit of alkaline phosphatase per 100 $\mu$g of DNA and then boiled for 10 min. The 8-hydroxy-2-deoxy guanosine (8-OH-dG) DNA damage assay was performed by using a commercially available kit (Cayman Chemical). The measurements are based on a competitive enzyme immunoassay between 8-OH-dG and an 8-OH-dG-acetylcholinesterase (AChE) conjugate (8-OH-dG tracer) with a limited amount of 8-OH-dG monoclonal antibody. After conjugation, Ellman's reagent (used to quantify the number or concentration of thiol groups) was used as a developing agent and read spectrophotometrically at 412 nm. The intensity measured was proportional to the amount of 8-OH-dG that was expressed in pg/ml.

### Large Amplicon quantitative PCR assay

For preparation of DNA, mouse skin tissues were minced and placed in a microfuge tube containing 0.5 ml lysis buffer (100 mM Tris/HCl pH 8.5, 5 mM EDTA, 0.2% SDS, 200 mM NaCl). Proteinase K was added at a final concentration of 100 mg/ml and incubated at 55 °C overnight. The lysate was extracted twice with an equal volume of phenol:chloroform:isoamyl alcohol (25:24:1, v/v) (GibcoBRL). DNA in the lysate was precipitated by addition of an equal volume of propan-2-ol. The DNA precipitates were solubilized in TE buffer (10 mM Tris/HCl, pH 8.0 and 1 mM EDTA). DNA purity and concentration were measured using a NanoDrop™ spectrophotometer (Thermo Scientific). Finally, DNA was digested with *Escherichia coli* formamidopyrimidine DNA glycosylase (Fpg) to cleave oxidized DNA bases and induce strand breaks with its associated AP lyase activity. To examine the formation of oxidative DNA damage in two mouse genes, polymerase $\beta$ (pol$\beta$) and $\beta$-globin, large Amplicon quantitative PCR (LA-qPCR) was performed as described earlier [17,18]. Briefly, a 6.5-kb long region of pol$\beta$ was amplified using the LongAmp Taq DNA polymerase (New England Biolabs) with the following primers: 5′-TATCTCTCTTCCTCTTCACTTCTCCCC-3′ and 5′-CGTGATGCCGCCGTTGAGGGTCTCC-3′. Preliminary experiments were carried out to ensure the linearity of PCR amplification with respect to the number of cycles and DNA concentration. A 250-bp fragment from pol$\beta$ was also amplified for normalization of the data obtained with the long fragment using the primers: 5′-TATGGACCCCCATGAGGAACA-3′ and 5′-AACCGTCGGCTAAAGACGTG-3′. Likewise, for the mouse $\beta$-globin gene, a long fragment of 8.7 kb was amplified using the primers 5′-TTGAGACTGTGATTGGCAATGCCT-3′ and 5′-CCTTTAATGCCCATCCCGGACT-3′, and normalized with a 200-bp short fragment using 5′-ACACTACTCAGAGTGAGACCCA-3′ and 5′-ATACCCAATGCTGGCTCCTG-3′. All of the amplified products were resolved and visualized using agarose gel electrophoresis and quantified using the VersaDoc system (Bio-Rad Laboratories). The relative amplification was normalized to the control values.

### Fluorescence activated cell sorting analysis

All anti-mouse antibodies for fluorescence activated cell sorting (FACS) and OneComp eBeads were purchased from eBioscience: Blocking CD16/CD32, for monocytes (CD11c PE-eFluor®610, IgG Isoytpe control PE-eFluor®610, Ly-6C APC, IgG1 K Isoytpe control APC), for neutrophils [Ly-6G(Gr-1) PerCP-Cyanine5.5, IgG2b K isotype PerCP-Cyanine5.5, CD11b PE-Cyanine7, IgG1 K Isoytpe control PE-Cyanine7], for macrophages (F4/80 FITC, IgG1 K isoytpe control FITC, CD11b PE-Cyanine7, IgG1 K Isoytpe control PE-Cyanine7). 7 mm wound with 3 mm surrounding tissue were collected at the given time points.

Wound tissues were then cut into small pieces with scissors and combined with 100 ml of collagenase/dispase (1 mg/ml) with RPMI medium and then incubated for 45 min at 37°C. The treated tissue/cell suspension was then passed through 18 and 20 gauge needles followed by straining using a 70 $\mu$m cell strainer (BD Bioscience). Cells were then washed with RPMI. The percoll gradient method was then used to separate neutrophils and monocytes/macrophages from the cell suspension. Collected cells were washed with RPMI and incubated in 10% purified CD16/CD32 in FACS buffer (10 $\mu$l) for 5 min to block non-specific binding to antibodies. Cells were then collected and re-suspended in 100 $\mu$l FACS buffer with 1 $\mu$l of each antibody and incubated on ice for 30 min and then followed by FACS analysis.

### Cytokine/chemokine levels

Skin and wound tissues were homogenized as described above. Millipore customized multiplex cytokine immunoassay was performed according to the manufacturers' protocol (Millipore) using equilibrated protein tissue homogenate. Level of the different analytes was quantified using a LuminexTM 200 instrument

 

(Millipore) by monitoring the fluorescence associated with the bead set.

### *In vivo* angiogenesis assay

The angiogenesis assay was done as previously described by us [19]. Briefly, the hair on the backs of control and THS-exposed mice was removed using Nair. The next day, they were injected subcutaneously with either insulin (Humulin) (1 $\mu$g/15 $\mu$l saline) or 15 $\mu$l saline using an insulin syringe. The injections were in well demarcated areas which were sufficiently separated to avoid interference. Both insulin and PBS were injected every 24 h for 4 days. The areas surrounding the injection sites were labelled using a permanent marker to ensure that the injections were always done at the same site. Skin samples from the injected areas were collected turned upside down and observed at day 5. Blood vessels were highlighted using ImageJ software and measured as previously described [19] (NIH).

### Immunolabelling procedure

Frozen sections were fixed in 4% paraformaldehyde for 20 min, rinsed with PBS, incubated in a solution of 0.1 M glycine in PBS for 20 min and blocked in 10% non-immune serum of the secondary antibody species in PBS containing 0.1% Triton X-100 for 30 min. Slides were then incubated for 2 h at room temperature with the primary antibodies in 1% BSA/PBS. The primary antibodies used, and respective dilutions, were the following: 1:200 FITC-labelled mouse anti-mouse $\alpha$-smooth muscle actin ($\alpha$SMA, Sigma–Aldrich) and 1:100 rabbit anti-mouse fibrinogen (Abcam). Sections were then washed three times with 0.1% BSA in PBS and incubated with 1:25 goat anti-rabbit secondary antibodies (Life Technologies), for 1 h at room temperature. After washing, sections were mounted in Vectashield containing DAPI (Vector Laboratories). Immunofluorescence was visualized and imaged using a Nikon Microphot-FXA fluorescence microscope with a Nikon DS-Fi1 digital camera and Nikon NIS-Elements software (Nikon Instruments).

### Statistical analysis

We used Graphpad Instat Software and Sigmaplot Software. ANOVA was used to test significance of group differences between two or more groups. In experiments with only two groups, we used a Student's *t* test.

## RESULTS

Studies performed in wound healing have focused on processes that occur later during healing. Reactive oxygen species (ROS) play the most crucial roles to put the healing on a path to repair or to impair healing. We have previously shown the importance of the early ROS markers and how they can lead to the prognosis of the development of impaired and chronic wounds [20,21]. Because production of ROS, release of cytokines/chemokines, influx of inflammatory cells, angiogenesis and collagen production, all occur during the early phases of healing, the parameters in the present study were focused on the first 7 days post-wounding.

### Impaired healing in THS-exposed mouse wounds

Wounds of control and THS-exposed mice were imaged periodically to record wound closure. The control wounds closed in approximately 12 days whereas the THS mouse wounds took an average 25% more time to heal (Figures 1A and 1B). In addition, after day 5 the wounds became more irregularly shaped, less contracted and the edges became thicker. To gain insight into the cellular changes leading to these differences, we performed histological examination of the wound tissue and found that the migration tongue in the wounds of the THS-exposed mice was virtually non-existent, the dermal–epidermal interactions were disrupted and the granulation tissue was poorly developed (Figure 2A). To further understand how these impaired THS wounds develop, we stained the tissue for fibrilar collagen to evaluate quality and spatial arrangement. Using the Masson Trichrome staining, we found that by day 7 the THS-exposed mouse wounds had considerably less staining in the granulation tissue, both in intensity and in area (Figure 2B). To determine whether the reduction in collagen deposition and in contraction was in part due to reduced numbers of myofibroblast (high producers of collagen), we stained day 7 wound tissues for $\alpha$SMA, a protein found in myofibroblasts. We found that there were significantly reduced numbers of myofibroblasts in the wounds of the THS-exposed mice when compared with the control mice, confirming deficiency in collagen deposition (Figure 2C). However, decreased collagen deposition has also been associated with presence of excessive proteases during healing. Matrix metalloproteinases (MMPs) are enzymes critical during different phases of wound healing, including keratinocyte migration that helps in reepithelization [22,23], and remodelling of the collagen in the granulation tissue [24]. Therefore, we examined the levels of two important MMPs in this process, MMP2 and MMP9. We found that the levels of active MMP2 in the THS-exposed mouse wounds is increased significantly at day 1 but then decreases at days 3–7 (Figure 3A, arrowhead). Levels of active MMP9, on the other hand, are higher up to day 3 in THS-exposed wounds and then decrease quickly by day 5 and 7 (Figure 3A, arrowhead).

Tissue inhibitors of matrix metalloproteinases (TIMPs) are known to play critical roles in maintaining the balance of active and inactive MMPs during the wound healing process [25]. TIMP-1 has been extensively shown to be associated with impaired and chronic wounds and its expression is widely observed during re-epithelialization near the leading edge of a normally healing wound, and it is also reduced when collagen is degraded in the granulation tissue [26–28]. Therefore, we examined the levels of TIMP-1 in the wounds of THS-exposed mice and found that the levels of TIMP-1 were significantly reduced, suggesting that in these wounds the proteases are not kept in check (Figure 3B).

Because our results on the MMPs did not appear to justify the destruction we see in the granulation tissue of THS-exposed mice, we examined the levels of another enzyme, elastase, that is also known to play a critical role in wound healing [29,30]. Elastin, the major target of elastase, confers elasticity on tissues. Elastase activity in the THS-exposed mouse wounds was significantly increased when compared with that in the wounds of the control mice (Figure 3C), suggesting that the granulation tissue of

 

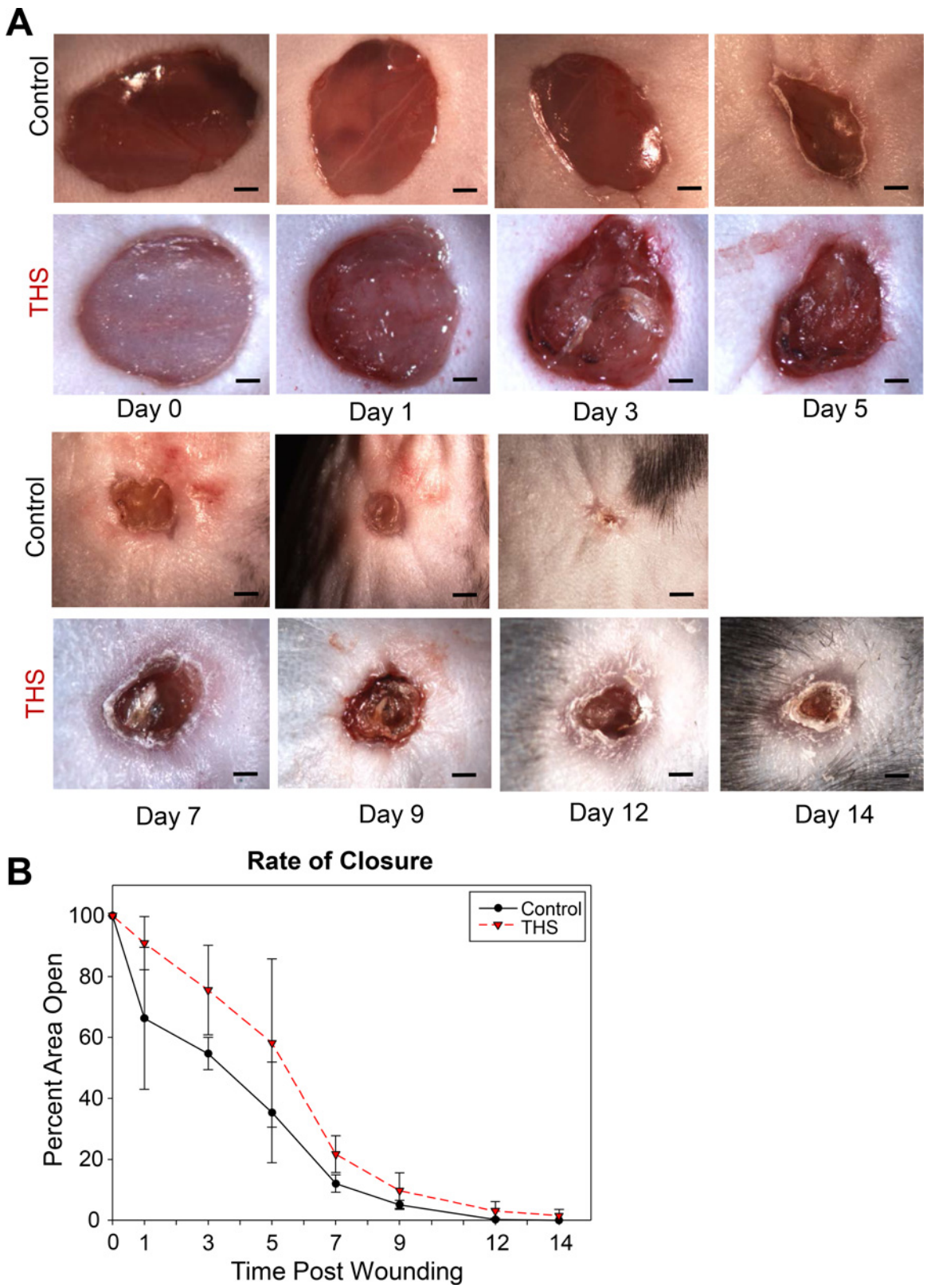


**Figure 1** **THS-exposed wounds have delayed wound closure**
(**A**) Wounds took longer to close in THS-exposed mice by approximately 25%. (**B**) Rate of wound healing was measured using ImageJ. Scale bar = 1 mm. All data are mean ± S.D. $n = 6$.

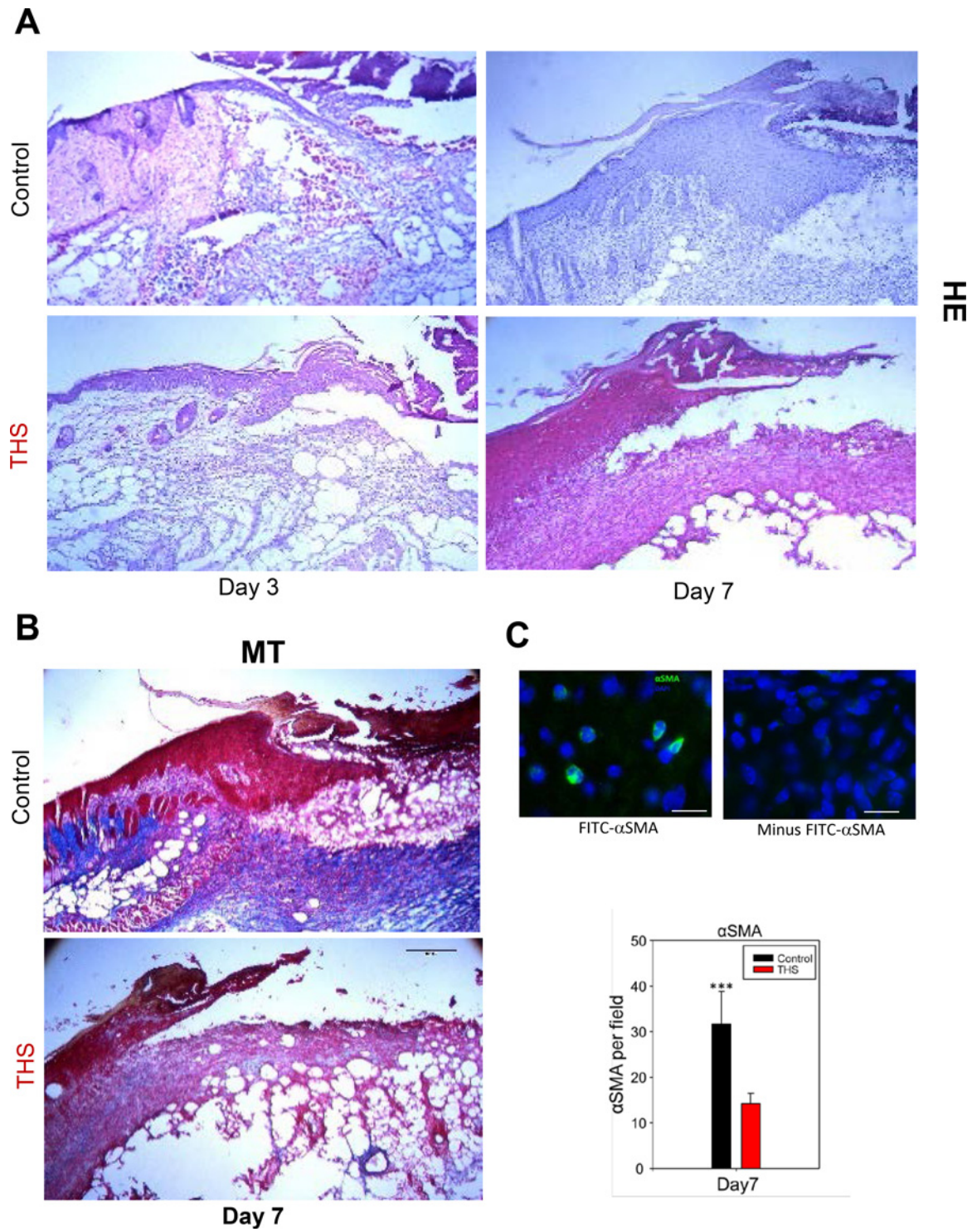


**Figure 2 Collagen deposition is impaired in THS-exposed wounds**

(**A**) Histological evaluation of control and THS-exposed wounds was performed by staining with haematoxylin and eosin (HE) at 3 and 7 days post-wounding. The migration tongue and the granulation tissue were disrupted in the THS-exposed mouse wound. (**B**) Wound sections at day 3 and 7 days post-wounding stained with Masson trichrome which stains the nuclei dark with Weigert's haematoxylin, the cytoplasm and muscle fibres red with Biebrich scarlet dye and the collagen blue with aniline blue dye. Collagen fibres are virtually absent from THS-exposed mouse wounds. (**C**) Myofibroblasts, producers of collagen, at day 7 post-wounding stained for $\alpha$SMA (green). The number of myofibroblasts is significantly decreased in THS-exposed mouse wounds. Scale bar = 20 $\mu$m. Data are mean $\pm$ S.D. $n = 5$. ***$P < 0.001$.

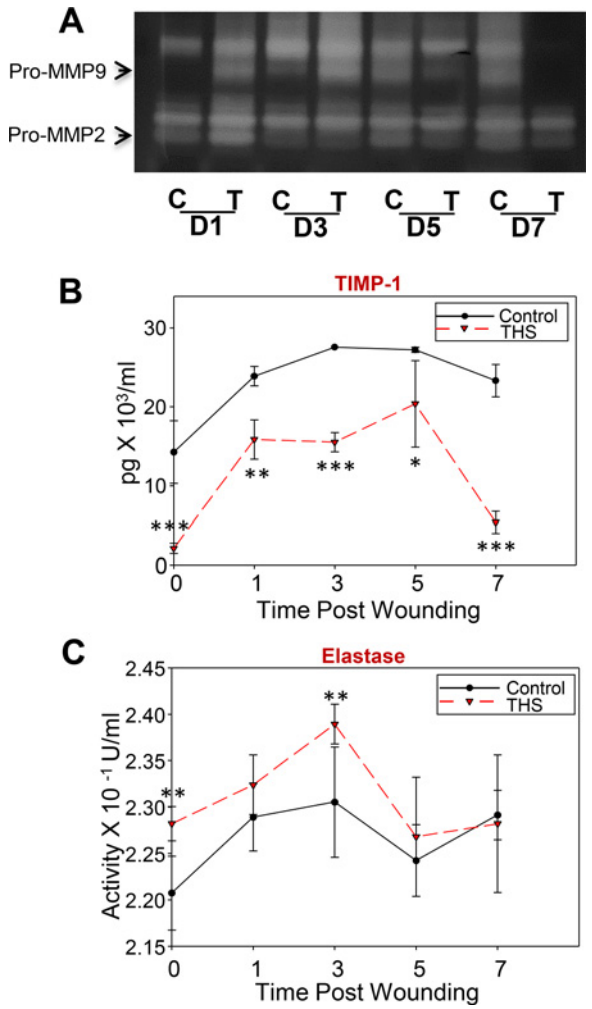


**Figure 3 THS-exposed mouse wounds have a high proteolytic microenvironment**

(**A**) Levels of MMP2 and 9 activity over time after wounding were measured by gelatine zymogram. (**B**) TIMP-1 levels were determined using a sandwich ELISA. TIMP-1 monoclonal antibody precoated wells were used to detect TIMP-1 in samples that were conjugated to a biotinylated detection polyclonal antibody specific for TIMP-1. (**C**) Elastase activity was measured using non-fluorescent substrate that upon digestion by elastase results in a fluorescent product measured at 530 nm. All data are mean ± S.D. $n = 6$. $^{*}P < 0.05$, $^{**}P < 0.01$, $^{***}P < 0.001$.

THS-exposed wound has lower elastic properties than normal and therefore might therefore be susceptible to reopening.

## THS wounds have redox imbalance during wound healing

One of the important parameters in wounds with impaired healing is the presence of an imbalanced redox state. To determine whether the impaired wounds of THS-exposed mice have altered oxidative stress levels, we examined several components of the oxidative stress cycle. SOD activity, an enzyme that is critical in the dismutation of superoxide anions to $H_2O_2$, was already greatly significantly elevated by 4 h post-wounding when compared with the control wounds (Figure 4A). These levels remained high during the first 7 days post-wounding. Consistent with the SOD activity, $H_2O_2$ levels were also significantly elevated in the THS-exposed mouse wounds (Figure 4B). Furthermore, we observed that unwounded skin in THS-exposed mice already has levels of $H_2O_2$ that are significantly higher than those in the skin of control mice, suggesting that the toxicants of THS affect the normal physiology of the skin and elevate stress levels even in the absence of wounding (Figure 4B). Catalase activity, one of the critical antioxidant enzymes that processes $H_2O_2$ into $H_2O$ and $O_2$ is not changed over the course of healing (Figure 4C). However, the activity of the other critical antioxidant enzyme, GPx, was greatly decreased during the first 3 days post-wounding (Figure 4D), suggesting significant reduction in antioxidant capacity in the wound tissue of THS-exposed mice.

The presence of oxidative stress can lead to significant molecular damage. We found that in THS-exposed mouse wounds there was a significant increase in the levels of MDA, a marker for lipid peroxidation, particularly after 5 days post-wounding (Figure 5A). This damage to lipids was particularly evident after 5 days post-wounding. Damage to proteins can occur by modification of tyrosine residues converting them to 3-nitrotyrosine (3-NT). The levels of 3-NT in the THS-exposed mouse wounds were significantly higher after 2 days post-wounding (Figure 5B). Another deleterious effect due to excessive oxidative stress occurs on DNA. 8-Hydroxylation of the guanine base (8-OH-dG) on DNA in the presence of oxidative stress, results in DNA damage. We show that the levels of 8-OH-dG in the THS-exposed mouse wounds were extremely high and much higher than the control during the entire period of healing (Figure 5C). Interestingly, we observed that the detrimental effects of oxidative stress observed in the wounds were also seen in unwounded skin of the THS-exposed mice (Figures 5A–5C).

To further confirm the genotoxic effect of THS we measured the oxidative stress-induced DNA damage using LA-qPCR. Genomic DNA was extracted as described in Research Design and Methods followed by the digestion with the *E. coli* formamidopyrimidine DNA glycosylase (Fpg) enzyme that acts on 8-oxoG and other oxidized lesions, and generates strand breaks at their sites. LA-qPCR is highly sensitive to oxidative DNA damage when coupled with the repair enzyme Fpg that is specific for incision of oxidized purine lesions. We amplified both the 6.5-kb DNA pol$\beta$ and 8.7-kb $\beta$-globin gene fragments with LA-qPCR. Short fragments (250–200 bp) in the same corresponding genes were also amplified under identical conditions and used for normalization of the long fragments. The intensity of the short fragments remained almost unchanged in both THS-exposed and control mouse samples, as much shorter regions of DNA would be relatively independent of oxidative DNA damage (Figures 5D and 5E). However, when compared with the controls, THS caused a marked reduction of the long amplification products for both genes, indicating the formation of oxidized DNA lesions. It can also be seen that the degree of such reduction varies in different mouse DNA samples, suggesting inter-individual differences in the formation and repair of oxidative DNA lesions. These results indicate that THS exposure causes increased levels of oxidative DNA damage in the mouse skin and in wounds.

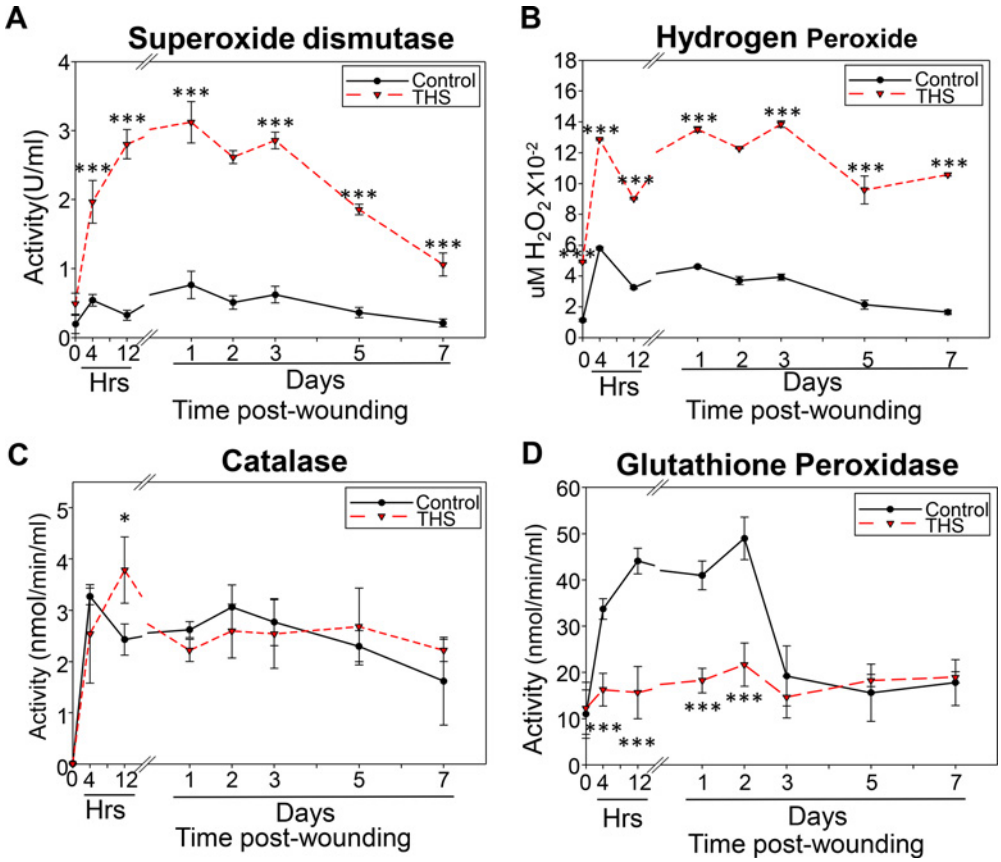


**Figure 4 Oxidative stress is elevated in THS-exposed mouse wounds**

(**A**) SOD activity was measured using tetrazolium salt detectible at 450 nm upon conversion into formazan dye. One unit of SOD is defined as the amount of enzyme needed to cause 50% dismutation of the superoxide radical. (**B**) $H_2O_2$ was measured using a non-fluorescent substrate 10-acetyl-3,7-dihydroxyphenoxazine that converts to fluorescent substance, resorufin, detectible at 530 nm/605 nm. (**C**) Catalase and methanol react to give rise to formaldehyde that further reacts with the chromogen, purpald, spectrophotometrically at 540 nm. (**D**) GPx activity was measured using a kinetic reactive measurement where GPx is the limiting reagent. Absorbance was read at 340 nm at 1 min intervals. All data are mean $\pm$ S.D. $n = 6$. $^*P < 0.05$, $^{***}P < 0.001$.

## THS exposure causes a dysfunctional immune response upon wounding

Proper wound healing results from the synchronized yet overlapping infiltration of inflammatory cells to the wound site. Disruption in the sequential entry of immune cells to sites of injury can lead to the impairment of wound closure and result in improper healing. The presence of inflammatory cells in the tissue was evaluated by flow cytometry. Singlet cell populations were defined by plotting forward scattered light height (FSC-H) compared with FSC area (Figure 6A and Supplementary Figure S1). The first cells to infiltrate the wound are the neutrophils which come into the tissue to kill bacteria. The number of neutrophils, defined by the markers Ly6G and CD11b (Figure 6A), was very similar in both control and THS-exposed mouse wounds (Figure 6B).

The wave of neutrophils is followed by monocytes. Monocytes play central roles in response to injury, inflammation and host defense because they differentiate into macrophages, which are critical for wound repair. We found that the presence of monocytes at the wound site, assessed by markers CD11c and Ly6C, was significantly delayed in the THS-exposed mouse wounds. It peaked at day 3 rather than day 1 post-wounding and decreased to control levels by day 5 much like the control (Figure 6C and Supplementary Figure S2). Macrophages remove and clear neutrophils and bacteria and elicit chemokines to recruit lymphocytes, and also stimulate the migration of fibroblast, epithelial and endothelial cells for the later phases of healing and remodelling. Using the macrophage markers F4/80 and CD11b, we found that, in the THS-exposed mice, the number of these leucocytes was significantly reduced during the first 5 days post-wounding (Figures 6A and 6D, Supplementary Figure S2), indicating that most monocytes do not differentiate into macrophages. These results strongly suggest that the microenvironment of the THS-exposed mouse wounds does not promote monocyte to macrophage differentiation, a critical aspect of the inflammatory response and that the macrophage inflammatory phase is defective.

## THS-exposed wounds display impaired production of chemokines

Chemotaxis of inflammatory and immune cells is heavily dependent on the expression and appropriate production of chemokines

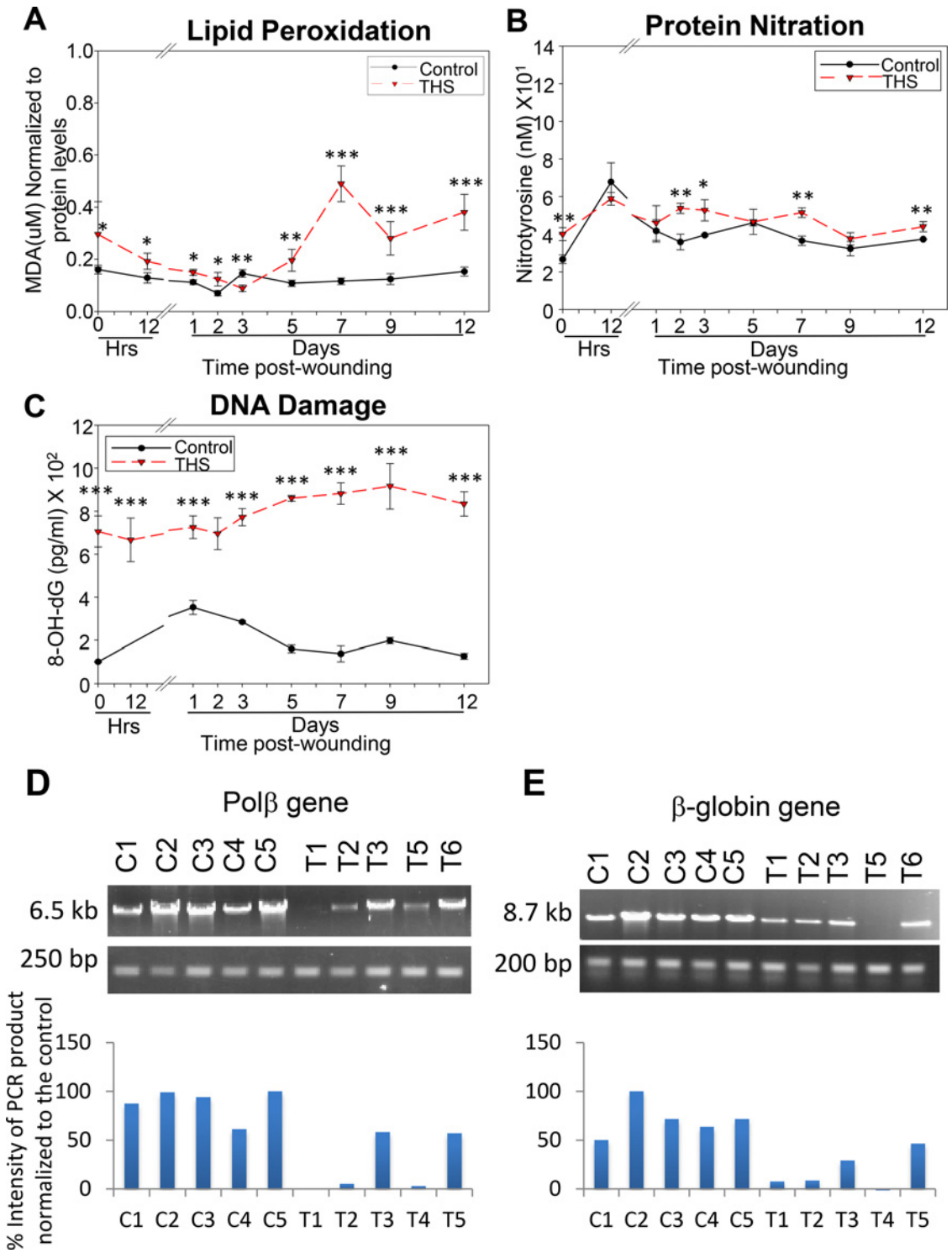


**Figure 5** **Stress related tissue damage occurs in skin and wounds of THS-exposed mice**

(**A**) Lipid peroxidation levels were fluorometrically measured at an Ex/Em of 540 nm/590 nm using TBARS. (**B**) Nitrotyrosine levels were evaluated using a competitive enzyme immunoassay. (**C**) 8-OH-dG levels were read spectrophotometrically at 412 nm using Ellman's reagent. (**D**) Formation of oxidative DNA damage in two mouse genes, pol$\beta$ and (**E**) $\beta$-globin, was performed by Long Amplicon-qPCR. Overall, oxidative stress-associated damage to tissue was increased in THS-exposed mouse wounds. All data are mean $\pm$ S.D. $n = 6$. *$P < 0.05$, **$P < 0.01$, ***$P < 0.001$.

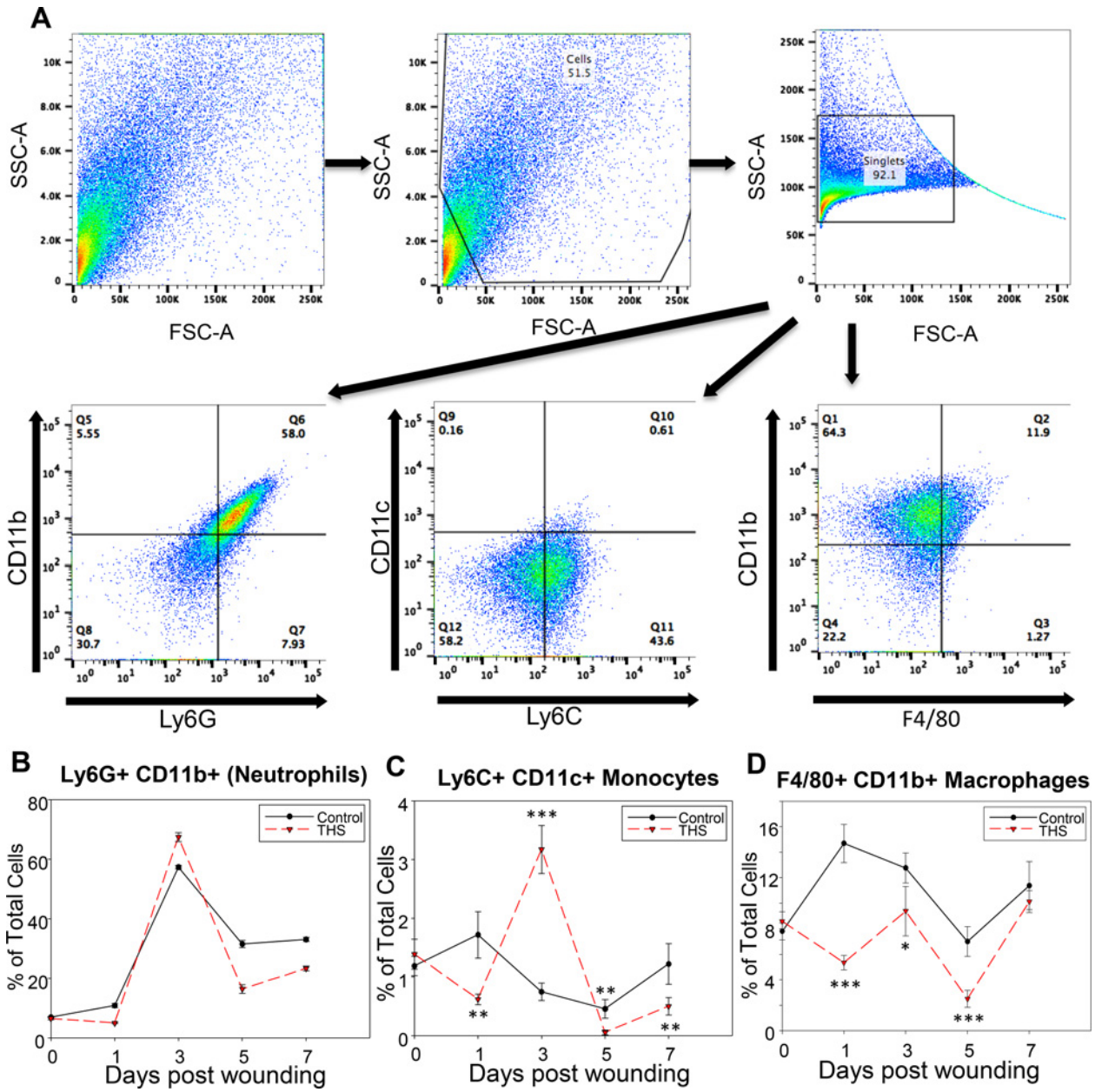


**Figure 6** **THS-exposure delays inflammatory response**

(**A**) Schematic of flow cytometry analysis of single cells isolated from THS-exposed and control mouse wounds at various time points. SSC-A is side scatter area, FSC-H is forward scatter height and FSC-A is forward scatter area. FACS was performed on wound cells immunolabelled and separated into neutrophils [CD11b PE-Cyanine7, Ly-6G (Gr-1) PerCP Cy5.5], monocytes (CD11c Alexa Fluor®532, Ly-6C APC), macrophages (F4/80 FITC, CD11b PE-Cyanine7). (**B**) Neutrophils were estimated as a percentage of total cell population isolated. (**C**) Monocytes were calculated as a percent of the total cell population isolated. (**D**) Percent cells with macrophage phenotype was calculated based on the total cell population. All data are mean ± S.D. $n = 5$. $^{*}P < 0.05$, $^{**}P < 0.01$, $^{***}P < 0.001$.

and cytokines during the course of wound healing [31,32]. To determine whether the altered number of inflammatory cells attracted to the wound site was in part due to an imbalance in the presence of chemokines/cytokine, we performed multiplex array cytokine analysis (Figure 7). Although KC, a major chemokine that chemoattracts neutrophils is lower in the THS-exposed mice (Figure 7A), another chemokine which also attracts neutrophils, LIX is at normal levels (Figure 7B), potentially explaining why we see no difference in the number of neutrophils in the THS-exposed mouse and those of the control (Figure 6B). However, neutrophil maturation is probably compromised because granulocyte colony stimulating factor (GCSF), a cytokine that is very important in neutrophil maturation and function, is significantly decreased in THS-exposed mouse wounds (Figure 7C).

We also found that a major monocyte recruiting chemokine, monocyte chemoattractant protein (MCP-1/CCL2) is reduced in THS-exposed mice (Figure 7D). However, the other major chemokine that attracts monocytes, macrophage inflammatory protein 1$\alpha$ (MIP-1$\alpha$/CCL3) is found at normal levels, therefore together they could contribute for the elevated presence of monocytes in the wound (Figure 7E) albeit with a delayed response because MIP-1$\alpha$/CXCL2 peaks at day 3 much like the monocytes (Figure 6C). We also found that the number of these monocytes that differentiates into macrophages is significantly decreased in the THS-exposed mouse wounds which correlates well with the lower levels of leukaemia inhibitory factor (LIF), a cytokine that has the ability to induce the terminal differentiation of myeloid cells such as monocyte/macrophages (Figure 7F). In addition, we found that the chemokine MIG/CXCL9 levels are higher in THS-exposed mouse wounds very early in the healing process (Figure 7G). This chemokine stimulates cellular and molecular mechanisms involved in wound tissue resolution and remodelling. Therefore, presence at high levels early in the wound is detrimental to healing.

### THS-exposed mouse wounds have leaky blood vessels

Angiogenesis is an important component in providing oxygen and nutrients to promote proper repair processes during wound healing. We first determined whether THS-exposed mice responded normally to the angiogenic factor insulin [33] by performing an *in vivo* angiogenesis assay. We found that injection of insulin subcutaneously resulted in the development of many sprouting microvessels in the skin of control mice but that insulin was unable to elicit sprouting of the blood vessels in the THS-exposed mouse skin (Figures 8A and 8B). Furthermore, we observed that the THS-exposed mouse skin blood vessels were leaky (Figure 8A). To determine whether blood vessel leakage was also observed during the wound healing process, we immunolabelled tissue sections from day 7 wounds for fibrinogen, a protein that is involved in clot formation and found that fibrinogen was present in the periphery of the blood vessels of THS-exposed mouse wounds, suggesting microvessel leakage (Figure 8C).

## DISCUSSION

First hand smoke (FHS) and second hand smoke (SHS) have previously been reported to cause impaired healing [34–37]. Doctors avoid performing surgery on patients who smoke due to known complications in clot formation, healing times and the quality of healing [12,38]. However, the effects of THS on healing are not well known. This is particularly important because THS is a stealth 'toxin' that permeates the homes of smokers and affects infants, children, spouses of smokers and elderly living in that environment. We have recently shown that THS has deleterious effects on multiple organs and also delays healing of skin wounds [14]. However, the underlying cell and molecular mechanisms that lead to THS-induced impaired healing are not known. In the present study we show that THS delays wound healing by delaying wound closure, increasing oxidative stress and its associated tissue damages, causing an imbalance in chemokines and cytokines that result in decreasing/delaying the inflammatory response, decreasing collagen deposition, decreasing angiogenesis and increasing blood vessel leakage and clot formation.

After wounding, re-epithelialization was followed over time and the area of the wounds measured. We found that THS delays wound closure; improper migration of the epithelial tongue and defective dermal epidermal interaction in conjunction with poor granulation tissue formation could be the reason for improper healing of the exposed mice. The epidermal cells do not form the normal epidermal tongue that moves over the granulation tissue to cover the wound and does not form adhesions with the underlying dermis as well as proper deposition of the basement membrane to establish firm connections.

Increased collagen deposition is critical for granulation tissue formation, and remodelling plays a critical role in providing the structural integrity to the healing tissue. The decrease in the level of collagen deposition observed at day 7 post-injury in the THS-exposed mouse wounds correlates with the significantly reduced number of myofibroblasts, cells that effectively produce fibrillar collagen [39]. Epithelial and stromal cells vital to the regenerative process in the wounded tissue have been shown to produce multiple MMPs [40,41]. Especially MMP2 and 9 have been shown to be localized to the epithelial–stromal interface behind the migrating epithelial cells, that suggest their role in remodelling of the stroma and reorganization of the basement membrane [42]. The levels of MMP2 and 9 which are very important in reepithelization and tissue remodelling [31,32], are elevated very early on and reduced at later time points in the wound tissue of THS-expose mice suggesting its role in impaired wound closure. Furthermore, lower levels of active MMP9, especially the reduction at day 7, correlate with delayed reepithelization and disorderly collagen fibrillogenesis [14,43]. Proper function of MMPs is, therefore, critical to correct tissue restoration processes.

TIMP-1, one of the four-member family of TIMPs, was significantly reduced in the wounds of THS-exposed mice. Previous studies have reported the family of TIMPs to have inhibitory actions on multiple MMPs [24]. However, the low levels of active MMP2 and 9 did not correlate with the lower levels of TIMP-1 we observed, suggesting that other TIMPs not included in our experiments might explain the low levels of MMP2 and 9. Furthermore, it is also possible that the increases in ROS levels we observe during the inflammatory phase of the THS-exposed mouse wounds could inhibit the pro-peptide cleavage by reacting with cysteine in the pro-peptide [44–46]. Additionally, the overall increase in elastase suggest a more proteolytic environment in the granulation tissue [30], which leads to elastin breakdown, a protein that is critical for elasticity of the healed tissue [47,48]. This might be one of the reasons why post-surgical wounds reopen in many smokers [49–51].

One of the primary responses during wound healing is the production of ROS; the imbalance in the levels of ROS is a critical factor in causing impaired wounds [52]. Significantly elevated SOD activity gives rise to increases in $H_2O_2$ that if not broken down to $H_2O$ and $O_2$ by the antioxidant enzymes, GPx and catalase, lead to increase in oxidative stress [53].

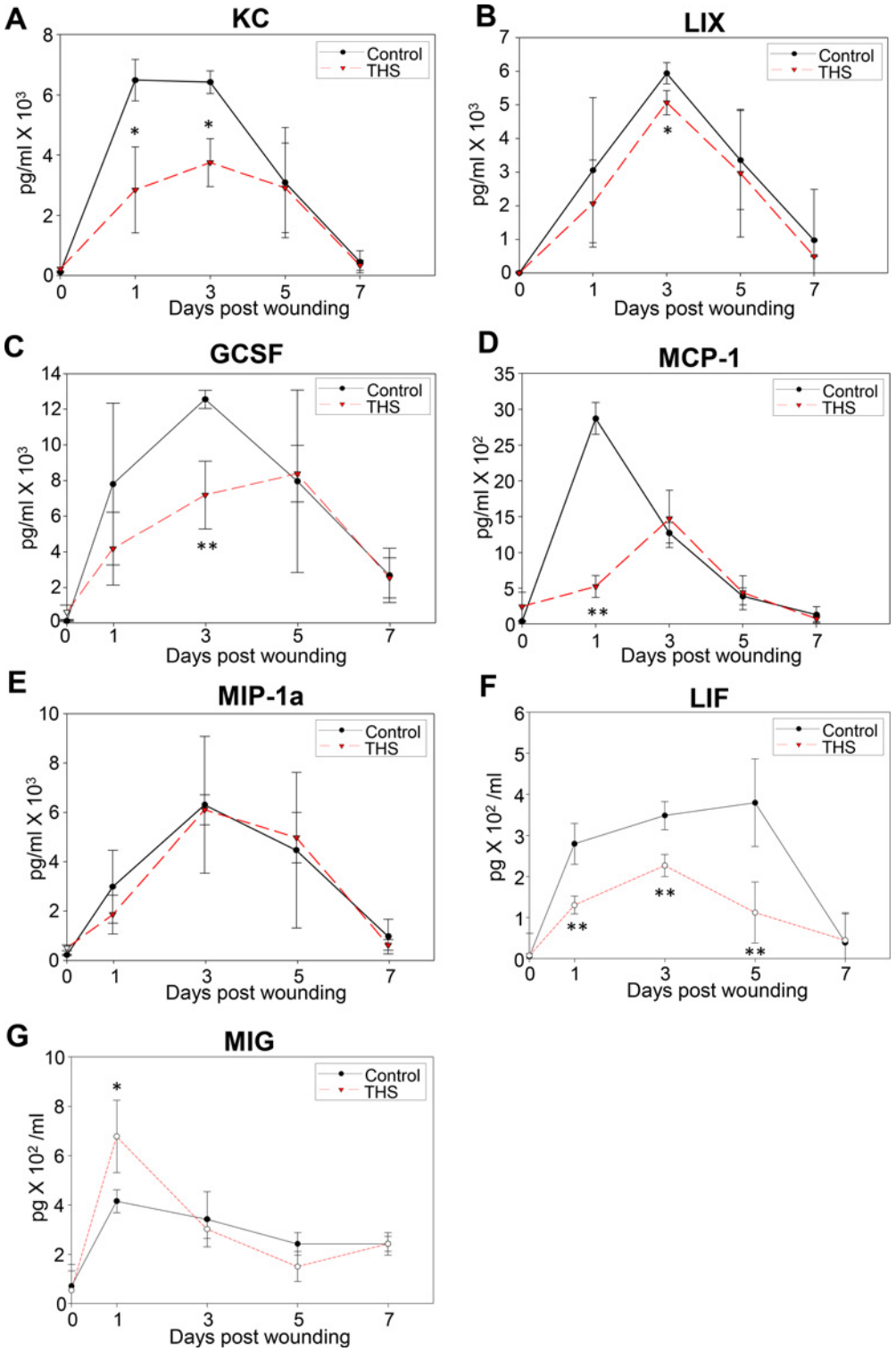


**Figure 7** **Chemokine and cytokine profile in THS-exposed mouse wounds**

(**A–G**) Wound tissue homogenates were analysed using a multipex cytokine array immunoassay and a LuminexTM 200 instrument to monitor fluorescence associated with magnetic beads. KC and LIX are chemoattracts for neutrophils, GCSF is involved in maturation of neutrophils, MCP-1 and MIP-1$\alpha$ are chemoattractants for monocytes, LIF is involved in differentiation of monocytes to macrophages and MIG is a chemokine involved in remodelling of the wound tissue. All data are mean $\pm$ S.D. $n = 3$. *$P < 0.05$, **$P < 0.01$.

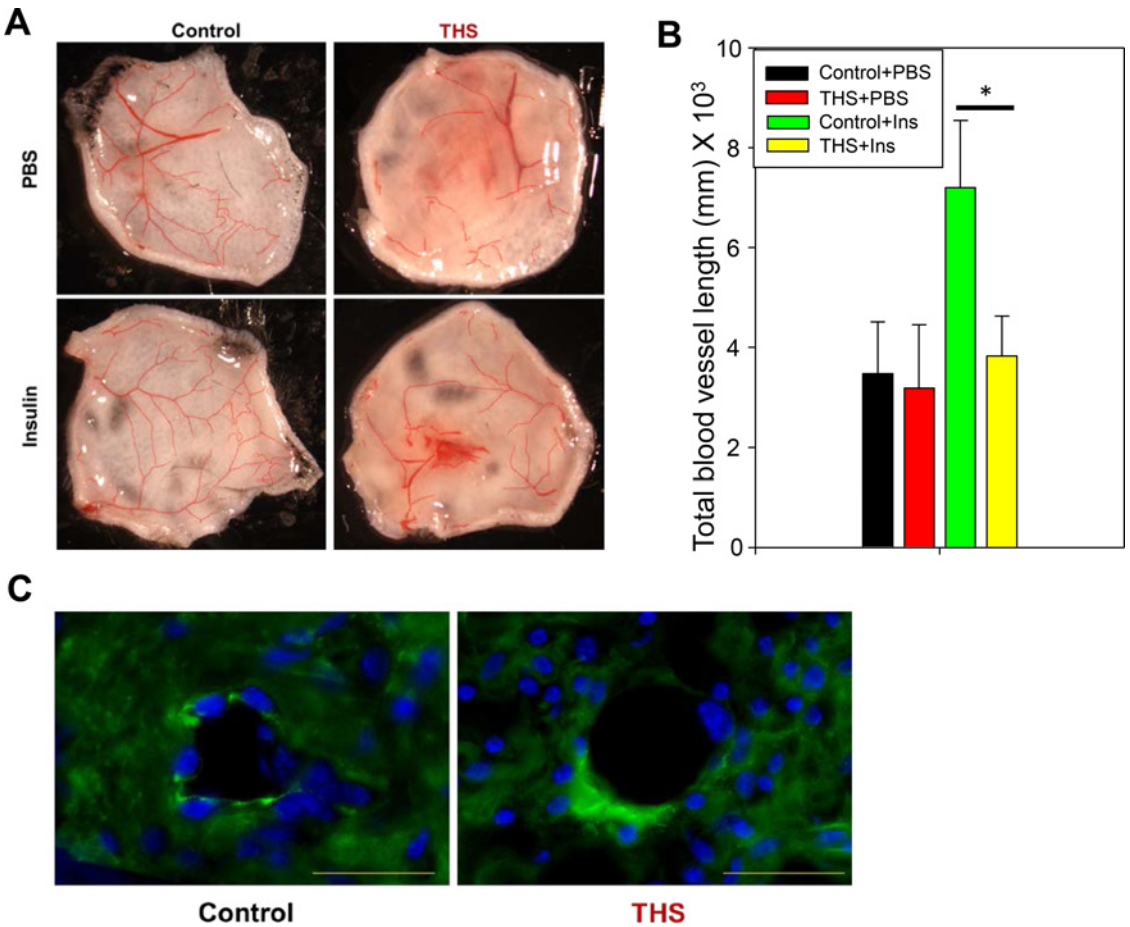


**Figure 8** **THS-exposure inhibits angiogenesis**

(**A**) Stimulation of angiogenesis upon insulin treatment was done by subcutaneous injection of 1 $\mu$g insulin and PBS independently for 4 days, followed by excision of the area of interest and (**B**) measuring the length of blood vessels. (**C**) Immunolabelling of control and THS-exposed mice wound sections at day 7 post-wounding for fibrinogen was done to show the presence of leaky blood vessels and fibrin cuffs. Scale = 50 $\mu$m. All data are mean $\pm$ S.D. $n = 4$. *$P < 0.05$.

Both superoxide anion and $H_2O_2$ can metabolize to result in peroxynitrite or hydroxyl radicals respectively which lead to oxidative damage. Molecules such as lipids, proteins and DNA are prime targets [20,54].

The significant increases in tissue damage observed in unwounded skin suggests that the THS toxins deposited on the skin lead to detrimental effects and also predispose the tissue to initiate a course of improper healing after injury. In particular, the DNA damage observed in the skin of the THS-exposed mice was very high suggesting that the cells are under significant stress from the smoke toxicants [18]. These results indicate that THS exposure causes increased levels of oxidative DNA damage in the mouse skin tissues, which is consistent with the observation that the skin from the same exposed mice exhibit higher levels of 8-OH-dG detected by both the TBARS and LA-qPCR assays [55].

The occurrence of sequential but overlapping inflammatory cascade is important for proper healing. The altered levels of monocytes and macrophages in the wound tissue of the THS-exposed mice suggest a disruption of the balance of influx of inflammatory cells. Furthermore, it has been suggested that macrophages in smokers, display defective capacity to kill [56]. Although we do see a spike in monocyte infiltration at day 3 post-wounding in the THS-exposed mouse wounds, the overall level of macrophages was significantly suppressed suggesting impaired maturation of monocytes to macrophages. These lower levels of macrophages could result in impairment of the clearance of dead neutrophils and of debris from the wound tissue and in altered production of factors that stimulate proper healing.

Because of the altered leucocyte levels in early wound healing we examined the chemokines and cytokines that lead to chemotaxis and maturation/function of these inflammatory cells. Although the levels of KC, chemoattractant for neutrophils [57,58], were reduced in the THS-exposed mouse wounds the levels of LIX/ENA-78, another chemokine that chemoattracts neutrophils was present at normal levels [59]. This explains the presence of similar numbers of neutrophils in the THS-exposed mouse wounds. However, we observed lower levels of GCSF, which

not only is a key regulator of neutrophil production [60] but also plays an essential role in neutrophil trafficking [61]. This suggests that although we detect similar numbers of neutrophils infiltrating the wound tissue in both THS-exposed and control mice, these neutrophils may not be fully functional. GCSF, also directly affects monocytes and modulates their cytokine secretion [62]. In the case of the monocytes we found that MCP-1/CCL2 was decreased at day 1 post-wounding which explains the delayed infiltration of monocytes we see [63]. However, the fact that the levels of MIP-1$\alpha$, another chemokine that attracts monocytes, are virtually the same in THS-exposed and in control mice and that the monocytes peak at day 3 post-wounding suggest that this chemokine plays a major role in the monocyte chemotaxis to the wound. Furthermore, we show that there is an overall reduced level of the interleukin 6 class protein LIF; this cytokine is critical for monocyte maturation into macrophage and for proper formation of the granulation tissue [64]. Another chemokine that plays a very important role in the resolution and remodelling of the healing process is MIG/CXCL9. In the THS-exposed mouse wounds [65] the levels of this chemokine are lower after 5 days post-wounding suggesting poor remodelling of the wound tissue.

Angiogenesis is required for proper nutrition and oxygenation of the wound tissue. Our observation that THS exposure results in the development of fewer blood vessels in response to an angiogenic molecule indicates that there is a deficiency in the ability of the endothelial cells to migrate to the wound site and form vessels. The lack of angiogenesis could also be due to the inability of the endothelial cells to adhere to each other and form tubes [66]. In support of the impaired adhesion are our findings that the vessels formed in the wounds of THS-exposed mice are leaky.

We delineate for the first time the mechanisms involved in THS-induced poor wound healing. They involve delayed rate of healing, increased oxidative stress, impaired inflammation, improper cytokine/chemokine balance and abnormal angiogenesis, driving the pathogenesis of impaired wound healing. These findings are also instrumental to understanding both FHS- and SHS-induced impaired healing. Taken together, our findings provide powerful insight into the role of tobacco smoke in wound healing and in particular targeting patients previously exposed to THS and undergoing surgery with substantial risk of developing difficult-to-treat surgical wounds.

## CLINICAL PERSPECTIVES

- The present study investigates the effects on wound healing of tobacco smoke toxins deposited on surfaces (THS) and seeks to understand the mechanisms of THS-induced impaired healing.
- We show that THS delays wound healing by, increasing oxidative stress and its associated tissue damage due to protein nitration, lipid peroxidation and DNA damage. THS exposure also causes imbalance in chemokines and cytokines that result in decrease/delay in the inflammatory response, decrease in collagen deposition, decrease in angiogenesis and increase in blood vessel leakage and clot formation. Moreover, elastase levels are elevated which reduces elastin, decreasing wound plasticity, which may be responsible for reopening of wounds.
- Our findings have implications for understanding how surgical wounds in smokers heal poorly and/or re-open. They also provide insight into the mechanisms by which SHS/THS exposure delays and impairs healing. This is particularly important for children and the elderly who are bystanders exposed to THS and who may be at extensive risk of developing difficult-to-treat surgical wounds.

### AUTHOR CONTRIBUTION

Sandeep Dhall and Manuela Martins-Green conceived and designed the experiments. Sandeep Dhall, Raquelle Alamat, Anthony Castro, Altaf Sarker, Bo Hang, Jian-Hua Mao and Manuela Martins-Green performed the experiments. Sandeep Dhall, Alex Chan and Manuela Martins-Green analysed the data. Manuela Martins-Green and Bo Hang contributed reagents/materials/analysis tools. Sandeep Dhall and Manuela Martins-Green wrote the manuscript.

### ACKNOWLEDGEMENTS

We thank Yagnika Patel for helping with wound area determination using ImageJ.

### FUNDING

This work was supported by the Tobacco Research Disease Related Program (TRDRP) [grant numbers 22RT-0121 and 23DT-0103 (to M.M.-G.)].

## REFERENCES

1 Guo, S. and Dipietro, L.A. (2010) Factors affecting wound healing. J. Dent. Res. **89**, 219–229 CrossRef PubMed
2 Sen, C.K., Gordillo, G.M., Roy, S., Kirsner, R., Lambert, L., Hunt, T.K., Gottrup, F., Gurtner, G.C. and Longaker, M.T. (2009) Human skin wounds: a major and snowballing threat to public health and the economy. Wound Repair. Regen. **17**, 763–771 CrossRef PubMed
3 Centers for Disease Control and Prevention (US), National Center for Chronic Disease Prevention and Health Promotion (US) and Office on Smoking and Health (US) (2010), How Tobacco Smoke Causes Disease: The Biology and Behavioral Basis for Smoking-Attributable Disease, Centers for Disease Control and Prevention (US), Atlanta, GA
4 Matt, G.E., Quintana, P.J.E., Destaillats, H., Gundel, L.A., Sleiman, M., Singer, B.C., Jacob, P., Benowitz, N., Winickoff, J.P., Rehan, V. et al. (2011) Thirdhand tobacco smoke: emerging evidence and arguments for a multidisciplinary research agenda. Environ. Health Perspect. **119**, 1218–1226 CrossRef PubMed
5 Winickoff, J.P., Friebely, J., Tanski, S.E., Sherrod, C., Matt, G.E., Hovell, M.F. and McMillen, R.C. (2009) Beliefs about the health effects of "thirdhand" smoke and home smoking bans. Pediatrics **123**, e74–e79 CrossRef PubMed
6 Sleiman, M., Gundel, L.A., Pankow, J.F., Jacob, P., Singer, B.C. and Destaillats, H. (2010) Formation of carcinogens indoors by surface-mediated reactions of nicotine with nitrous acid, leading to potential thirdhand smoke hazards. Proc. Natl. Acad. Sci. U.S.A. **107**, 6576–6581 CrossRef PubMed

 

7 Burton, A (2011) Does the smoke ever really clear? Thirdhand smoke exposure raises new concerns. Environ. Health Perspect. **119**, A70–A74 CrossRef PubMed
8 Mosely, L.H. and Finseth, F. (1977) Cigarette smoking: impairment of digital blood flow and wound healing in the hand. Hand **9**, 97–101 CrossRef PubMed
9 Rogers, R.L. (1983) Cigarette smoking decreases cerebral blood flow suggesting increased risk for stroke. J. Am. Med. Assoc. **250**, 2796 CrossRef
10 Waeber, B., Schaller, M.D., Nussberger, J., Bussien, J.P., Hofbauer, K.G. and Brunner, H.R. (1984) Skin blood flow reduction induced by cigarette smoking: role of vasopressin. Am. J. Physiol. Hear Circ. Physiol. **247**, H895–H901
11 Thomsen, T., Tønnesen, H. and Møller, A.M. (2009) Effect of preoperative smoking cessation interventions on postoperative complications and smoking cessation. Br. J. Surg. **96**, 451–461 CrossRef PubMed
12 Sorensen, L.T., Karlsmark, T. and Gottrup, F. (2003) Abstinence from smoking reduces incisional wound infection: a randomized controlled trial. Ann. Surg. **238**, 1–5 PubMed
13 Sorensen, L.T. and Jorgensen, T Short-term pre-operative smoking cessation intervention does not affect postoperative complications in colorectal surgery: a randomized clinical trial. Color Dis **5**, 347–352 CrossRef
14 Martins-Green, M., Adhami, N., Frankos, M., Valdez, M., Goodwin, B., Lyubovitsky, J., Dhall, S., Garcia, M., Egiebor, I., Martinez, B. et al. (2014) Cigarette smoke toxins deposited on surfaces: implications for human health. PLoS One **9**, e86391 CrossRef PubMed
15 Dhall, S., Wijesinghe, D.S., Karim, Z.A., Castro, A., Vemana, H.P., Khasawneh, F.T., Chalfant, C.E. and Martins-Green, M. (2015) Arachidonic acid-derived signaling lipids and functions in impaired healing. Wound Repair Regen **23**, 644–656 CrossRef PubMed
16 Petreaca, M.L., Do, D., Dhall, S., McLelland, D., Serafino, A., Lyubovitsky, J., Schiller, N. and Martins-Green, M. (2012) Deletion of a tumor necrosis superfamily gene in mice leads to impaired healing that mimics chronic wounds in humans. Wound Repair Regen **20**, 353–366 CrossRef PubMed
17 Furda, A., H. Santos, J. and Van Houten, B. (2014) Quantitative PCR-based measurement of nuclear and mitochondrial DNA damage and repair in mammalian cells. Methods Mol. Biol. **1105**, 419–437 CrossRef PubMed
18 Hang, B., Sarker, A.H., Havel, C., Saha, S., Hazra, T.K., Schick, S., Jacob, P., Rehan, V.K., Chenna, A., Sharan, D. et al. (2013) Thirdhand smoke causes DNA damage in human cells. Mutagenesis **28**, 381–391 CrossRef PubMed
19 Dhall, S., Silva, J.P., Liu, Y., Hrynyk, M., Garcia, M., Chan, A., Lyubovitsky, J., Neufeld, R.J. and Martins-Green, M. (2015) Release of insulin from PLGA-alginate dressing stimulates regenerative healing of burn wounds in rats. Clin. Sci. (Lond) **129**, 1115–1129 CrossRef PubMed
20 Dhall, S., Do, D., Garcia, M., Wijesinghe, D.S., Brandon, A., Kim, J., Sanchez, A., Lyubovitsky, J., Gallagher, S., Nothnagel, E.A. et al. (2014) A novel model of chronic wounds: importance of redox imbalance and biofilm-forming bacteria for establishment of chronicity. PLoS One **9**, e109848 CrossRef PubMed
21 Dhall, S., Do, D.C., Garcia, M., Kim, J., Mirebrahim, S., Lonardi, S., Nothnagel, E.A., Schiller, N. and Martins-Green, M. (2014) Generating and reversing chronic wounds in diabetic mice by manipulating wound redox parameters. J. Diabetes Res. **2014**, 562625 CrossRef PubMed
22 McCawley, L.J., O'Brien, P. and Hudson, L.G. (1998) Epidermal growth factor (EGF)- and scatter factor/hepatocyte growth factor (SF/HGF)mediated keratinocyte migration is coincident with induction of matrix metalloproteinase (MMP)-9. J. Cell Physiol. **176**, 255–265 CrossRef PubMed
23 Stevens, L.J. and Page-McCaw, A. (2012) A secreted MMP is required for reepithelialization during wound healing. Mol. Biol. Cell **23**, 1068–1079 CrossRef PubMed
24 Caley, M.P., Martins, V.L.C. and O'Toole, E.A. (2015) Metalloproteinases and wound healing. Adv. Wound Care **4**, 225–234 CrossRef
25 Vaalamo, M., Leivo, T. and Saarialho-Kere, U. (1999) Differential expression of tissue inhibitors of metalloproteinases (TIMP-1, -2, -3, and -4) in normal and aberrant wound healing. Hum. Pathol. **30**, 795–802 CrossRef PubMed
26 Vaalamo, M., Weckroth, M., Puolakkainen, P., Kere, J., Saarinen, P., Lauharanta, J. and Saarialho-Kere, U.K. (1996) Patterns of matrix metalloproteinase and TIMP-1 expression in chronic and normally healing human cutaneous wounds. Br. J. Dermatol. **135**, 52–59 CrossRef PubMed
27 Ashcroft, G.S., Herrick, S.E., Tarnuzzer, R.W., Horan, M.A., Schultz, G.S. and Ferguson, M.W.J. (1997) Human ageing impairs injury-induced *in vivo* expression of tissue inhibitor of matrix metalloproteinases (TIMP)-1 and -2 proteins and mRNA. J. Pathol. **183**, 169–176 CrossRef PubMed
28 Ladwig, G.P., Robson, M.C., Liu, R.A.N. and Kuhn, M.A.N.N. (2002) Ratios of activated matrix metalloproteinase-9 to tissue inhibitor of matrix metalloproteinase-1 in wound fluids are inversely correlated with healing of pressure ulcers. Wound Repair. Regen. **10**, 26–37 CrossRef PubMed
29 Grinnell, F. and Zhu, M. (1996) Fibronectin degradation in chronic wounds depends on the relative levels of elastase, 1-proteinase inhibitor, and 2-macroglobulin. J. Invest. Dermatol. **106**, 335–341 CrossRef PubMed
30 McCarty, S.M., Cochrane, C.A., Clegg, P.D. and Percival, S.L. (2012) The role of endogenous and exogenous enzymes in chronic wounds: a focus on the implications of aberrant levels of both host and bacterial proteases in wound healing. Wound Repair. Regen. **20**, 125–136 CrossRef PubMed
31 Gauglitz, G.G., Song, J., Herndon, D.N., Finnerty, C.C., Boehning, D., Barral, J.M. and Jeschke, M.G. (2008) Characterization of the inflammatory response during acute and post-acute phases after severe burn. Shock **30**, 503–507 CrossRef PubMed
32 Fivenson, D.P., Faria, D.T., Nickoloff, B.J., Poverini, P.J., Kunkel, S., Burdick, M. and Strieter, R.M. (1997) Chemokine and inflammatory cytokine changes during chronic wound healing. Wound Repair Regen **5**, 310–322 CrossRef PubMed
33 Liu, Y., Petreaca, M. and Martins-Green, M. (2009) Cell and molecular mechanisms of insulin-induced angiogenesis. J. Cell Mol. Med. **13**, 4492–4504 CrossRef PubMed
34 Ma, C. and Martins-Green, M. (2009) Second-hand cigarette smoke inhibits wound healing of the cornea by stimulating inflammation that delays corneal reepithelialization. Wound Repair Regen. **17**, 387–396 CrossRef PubMed
35 Wong, L.S. and Martins-Green, M. (2004) Firsthand cigarette smoke alters fibroblast migration and survival: Implications for impaired healing. Wound Repair Regen. **12**, 471–484 CrossRef PubMed
36 Guo, S. and Dipietro, L.A. (2010) Factors affecting wound healing. J. Dent. Res. **89**, 219–229 CrossRef PubMed
37 Jones, J. and Triplett, R. (1992) The relationship of cigarette smoking to impaired intraoral wound healing: a review of evidence and implications for patient care. J. Oral Maxillofac. Surg. **50**, 237–239 CrossRef PubMed
38 Hunt, T.K., Hopf, H. and Hussain, Z. (2000) Physiology of wound healing. Adv. Skin Wound Care **13** 2 Suppl, 6–11 PubMed
39 Asakura, T., Ishii, Y., Chibana, K. and Fukuda, T. (2004) Leukotriene D4 stimulates collagen production from myofibroblasts transformed by TGF-beta. J. Allergy Clin. Immunol. **114**, 310–315 CrossRef PubMed
40 Inoue, M., Kratz, G., Haegerstrand, A. and Ståhle-Bäckdahl, M. (1995) Collagenase expression is rapidly induced in wound-edge keratinocytes after acute injury in human skin, persists during healing, and stops at re-epithelialization. J. Invest. Dermatol. **104**, 479–483 CrossRef PubMed
41 Gill, S.E. and Parks, W.C. (2009) Metalloproteinases and their inhibitors: regulators of wound healing. Int. J. Biochem. **40**, 1334–1347 CrossRef


 

42 Mulholland, B., Tuft, S.J. and Khaw, P.T. (2005) Matrix metalloproteinase distribution during early corneal wound healing. Eye (Lond) **19**, 584–588 CrossRef PubMed

43 Kyriakides, T.R., Wulsin, D., Skokos, E.A., Fleckman, P., Shipley, J.M., Senior, R.M. and Bornstein, P. (2009) Mice that lack matrix metalloproteinase-9 display delayed wound healing associated with delayed reepithelization and disordered collagen fibrillogenesis. Matrix Biol **28**, 65–73 CrossRef PubMed

44 Fu, X., Kao, J.L.F., Bergt, C., Kassim, S.Y., Huq, N.P., D'Avignon, A., Parks, W.C., Mecham, R.P. and Heinecke, J.W. (2004) Oxidative cross-linking of tryptophan to glycine restrains matrix metalloproteinase activity: Specific structural motifs control protein oxidation. J. Biol. Chem. **279**, 6209–6212 CrossRef PubMed

45 Peppin, G.J. and Weiss, S.J. (1986) Activation of the endogenous metalloproteinase, gelatinase, by triggered human neutrophils. Proc. Natl. Acad. Sci. U.S.A. **83**, 4322–4326 CrossRef PubMed

46 Gu, Z. (2002) S-Nitrosylation of matrix metalloproteinases: signaling pathway to neuronal cell death. Science **297**, 1186–1190 CrossRef PubMed

47 Raghunath, M., Bächi, T., Meuli, M., Altermatt, S., Gobet, R., Bruckner-Tuderman, L. and Steinmann, B. (1996) Fibrillin and elastin expression in skin regenerating from cultured keratinocyte autografts: morphogenesis of microfibrils begins at the dermo-epidermal junction and precedes elastic fiber formation. J. Invest. Dermatol. **1996**, 1090–1095 CrossRef

48 Almine, J.F., Wise, S.G. and Weiss, A.S. (2012) Elastin signaling in wound repair. Birth Defects Res. C Embryo Today **96**, 248–257 CrossRef PubMed

49 Siana, J.E., Rex, S. and Gottrup, F. (1989) The effect of cigarette smoking on wound healing. Scand. J. Plast. Reconstr. Surg. Hand Surg. **23**, 207–209 PubMed

50 Jorgensen, L.N., Kallehave, F., Christensen, E., Siana, J.E. and Gottrup, F. (1998) Less collagen production in smokers. Surgery **123**, 450–455 CrossRef PubMed

51 Sherwin, M.A. and Gastwirth, C.M. (1990) Detrimental effects of cigarette smoking on lower extremity wound healing. J. Foot. Surg. **29**, 84–87 PubMed

52 Schäfer, M. and Werner, S. (2008) Oxidative stress in normal and impaired wound repair. Pharmacol. Res. **58**, 165–171 CrossRef PubMed

53 Buettner, G.R. (2011) Superoxide dismutase in redox biology: the roles of superoxide and hydrogen peroxide. Anticancer Agents Med. Chem. **11**, 341–346 CrossRef PubMed

54 Salvemini, D., Doyle, T.M. and Cuzzocrea, S. (2006) Superoxide, peroxynitrite and oxidative/nitrative stress in inflammation. Biochem. Soc. Trans. **34**, 965–970, (Pt 5) CrossRef PubMed

55 Sarker, A.H., Chatterjee, A., Williams, M., Lin, S., Havel, C., Jacob, P., Boldogh, I., Hazra, T.K., Talbot, P. and Hang, B. (2014) NEIL2 protects against oxidative DNA damage induced by sidestream smoke in human cells. PLoS One **9**, e90261 CrossRef PubMed

56 Holt, P.G. (1987) Immune and inflammatory function in cigarette smokers. Thorax **42**, 241–249 CrossRef PubMed

57 Xu, Q., Seemanapalli, S.V., Reif, K.E., Brown, C.R. and Liang, F.T. (2007) Increasing the recruitment of neutrophils to the site of infection dramatically attenuates *Borrelia burgdorferi* infectivity. J. Immunol. **178**, 5109–5115 CrossRef PubMed

58 Ritzman, A.M., Hughes-Hanks, J.M., Blaho, V.a., Wax, L.E., Mitchell, W.J. and Brown, C.R. (2010) The chemokine receptor CXCR2 ligand KC (CXCL1) mediates neutrophil recruitment and is critical for development of experimental lyme arthritis and carditis. Infect. Immun. **78**, 4593–4600 CrossRef PubMed

59 Walz, B.A., Burgener, R., Car, B., Baggiolini, M., Kunkel, S.L. and Strieter, R.M. (1991) Structure and neutrophil-activating properties of a novel inflammatory peptide (ENA-78) with homology to interleukin 8. J. Exp. Med. **174**, 1355–1362 CrossRef PubMed

60 Roberts, A.W. (2005) G-CSF: a key regulator of neutrophil production, but that's not all!. Growth Factors **23**, 33–41 CrossRef PubMed

61 Semerad, C.L., Liu, F., Gregory, A.D., Stumpf, K. and Link, D.C. (2002) G-CSF is an essential regulator of neutrophil trafficking from the bone marrow to the blood. Immunity **17**, 413–423 CrossRef PubMed

62 Saito, M., Kiyokawa, N., Taguchi, T., Suzuki, K., Sekino, T., Mimori, K., Suzuki, T., Nakajima, H., Katagiri, Y.U., Fujimura, J. et al. (2002) Granulocyte colony-stimulating factor directly affects human monocytes and modulates cytokine secretion. Exp. Hematol. **30**, 1115–1123 CrossRef PubMed

63 Deshmane, S.L., Kremlev, S., Amini, S. and Sawaya, B.E. (2009) Monocyte chemoattractant protein-1 (MCP-1): an overview. J. Interferon Cytokine Res. **29**, 313–326 CrossRef PubMed

64 Nicola, N.A. and Babon, J.J. (2015) Leukemia inhibitory factor (LIF). Cytokine Growth Factor Rev **26**, 533–544 CrossRef PubMed

65 Engelhardt, E., Toksoy, A., Goebeler, M., Debus, S., Bröcker, E.B. and Gillitzer, R. (1998) Chemokines IL-8, GROalpha, MCP-1, IP-10, and Mig are sequentially and differentially expressed during phase-specific infiltration of leukocyte subsets in human wound healing. Am. J. Pathol. **153**, 1849–1860 CrossRef PubMed

66 Eliceiri, B.P. and Cheresh, D.A. (2001) Adhesion events in angiogenesis. Curr. Opin. Cell Biol. **13**, 563–568 CrossRef PubMed


**Received 29 March 2016/25 April 2016; accepted 28 April 2016**

**Accepted Manuscript online 28 April 2016, doi: 10.1042/CS20160236**

 